SIMULATIONS OF THE SCALED REACTOR CAVITY COOLING SYSTEM EXPERIMENTAL FACILITY WITH FLOWNEX

A Thesis

by

MARCOS SALOMAO DE SENA

Submitted to the Graduate and Professional School of
Texas A&M University
in partial fulfillment of the requirements for the degree of

MASTER OF SCIENCE

Chair of Committee,	Yassin A. Hassan
Committee Members,	Maria King
	Rodolfo Vaghetto
Head of Department,	Michael Nastasi

August 2023

Major Subject: Nuclear Engineering

ABSTRACT

The scaled Water-cooled Reactor Cavity Cooling System (WRCCS) experimental facility reproduces a passive safety feature to be implemented in Generation IV nuclear reactors. It keeps the reactor cavity and other internal structures in operational conditions by removing heat leakage from the reactor pressure vessel. The present work used Flownex to model the facility and predict the experimental thermal-hydraulic behavior. Three representative steady-state cases defined by the bulk volumetric flow rate were simulated (*Re* = 2,409, *Re* = 2,490, and *Re* = 11,524). Flownex predictions of the cavity outlet temperature, risers' temperature profile and flow rate split were compared with the experimental data and previous RELAP simulations. The comparisons are in reasonable agreement with previous studies, demonstrating the ability of Flownex to simulate the RCCS behavior. For the low *Re* cases, temperature and flow split across the risers are evenly distributed. Conversely, there's an asymmetry trend in both temperature and flow distributions for the high *Re* case. Additionally, a sensitivity analysis was performed using the *Re* = 2,409 case to assess the impact on the system's temperature and flow due to power reduction transferred to the risers. The results showed very good adherence to the RELAP studies. Finally, a loss of secondary coolant scenario was conducted. Although Flownex employs a two-phase homogeneous mixture model, the global behavior of the average system's parameters reasonably agrees with predictions by previous studies in RELAP.

CONTRIBUTORS AND FUNDING SOURCES

Contributors

This work was supported by a thesis committee consisting of Professor Yassin A. Hassan (my advisor) and Professor Rodolfo Vaghetto, both from the Department of Nuclear Engineering, and Professor Maria King of the Department of Biological & Agricultural Engineering.

Funding Sources

All my graduate study has been supported by a scholarship from the Brazilian Navy.

NOMENCLATURE

AGR	Advanced Gas-cooled Reactor
CANDU	Canada Deuterium Uranium Reactor
CFD	Computer Fluid Dynamic
Gen I	Generation I Reactors
Gen II	Generation II Reactors
Gen III	Generation III Reactors
Gen IV	Generation IV Reactors
IEA	International Energy Agency
LWR	Light Water Reactor
OF-DTS	Optical Fiber Distributed Temperature Sensor
PIV	Particle Image Velocimetry
RCCS	Reactor Cavity Cooling System
RELAP	Reactor Excursion and Leak Analysis Program
Re	Reynolds Number
RPV	Reactor Pressure Vessel
RTD	Resistance Temperature Detector
TAMU	Texas A&M University
VHTR	Very High Temperature Reactor
WRCCS	Water-cooled Reactor Cavity Cooling System

TABLE OF CONTENTS

Page

LIST OF FIGURES

Page

LIST OF TABLES

Page

1. INTRODUCTION

Electricity plays an essential role in human life as it is inherently linked with technological development and fills the demand of energy for everyday needs: heating, cooling, cooking, mobility, and lighting [1]. Electricity represents up to 20% of the final energy consumption and demand has been increasing steadily in recent decades [1].

Yet, there are billions of people around the world, mostly from emerging markets and developing countries, that do not have access to modern electric devices which in turn will contribute to pushing energy demand up in the future decades [1]. By 2050, final energy consumption is expected to increase by about 30% and electricity production is projected to double [2].

In addition to this challenging scenario the International Energy Agency (IEA) Net Zero CO_2 Report addressing climate change mitigation urges for the use of technologies that meet the goal to reach zero carbon emissions by 2050 [2]. Contributing to this effort, nuclear power reactors have prevented more than 60 gigatons of CO_2 emissions over the past 50 years [2].

However, as a significant number of first- and second-generation nuclear reactors approximate their lifetime ending in the near future, new sustainable nuclear technologies must be developed and deployed to continue to address the increasing need for clean energy.

The generation of nuclear power plants is a methodology commonly used to subdivide the maturity of this kind of technology. There are four groups, as follows [3]:

- Generation I (Gen I)
- Generation II (Gen II)
- Generation III/III+ (Gen III/III+)
- Generation IV (Gen IV)

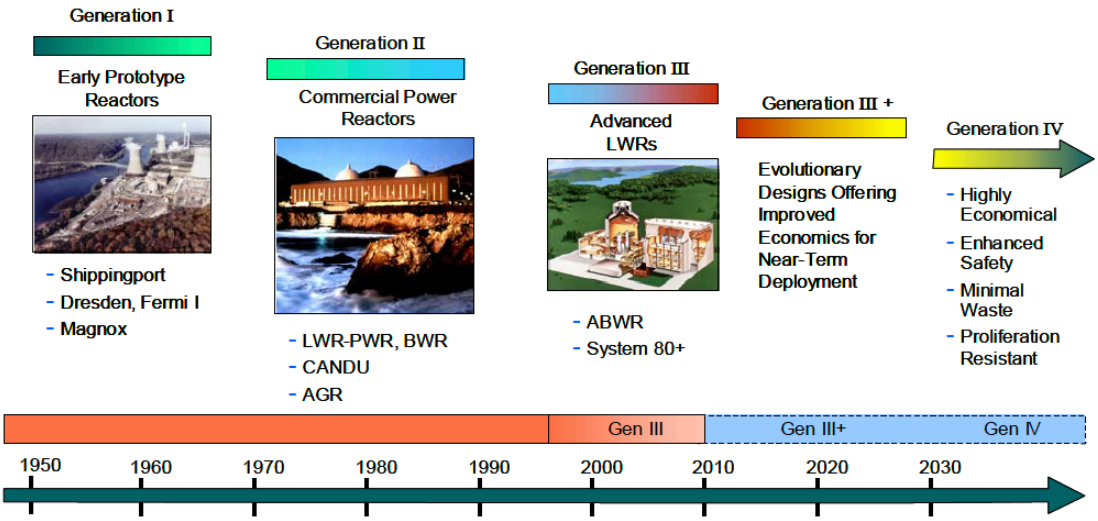

Figure 1. Generations of nuclear reactors. Reprinted from [3].

The first-generation accounts for the early prototype reactors and they represent the very first attempt to apply nuclear power technology for civilian purposes. Gen II consists of large commercial nuclear reactors with a lifetime of over 40 years. Many are still in operation, and they have safety features that improve reliability. Among the Gen II nuclear reactors are the well-known Light Water Reactor (LWR), Advanced Gas-cooled Reactor (AGR), and Canada Deuterium Uranium Reactor (CANDU).

The third generation was conceived in the 1990s and implements several improvements to the previous generation, especially in fuel technology, thermal efficiency, modularized construction, safety systems, and standardized designs. Gen III+ includes additional safety functions by applying passive systems that allow the reactor to be controlled without external intervention.

Reactors from the fourth generation are a group of 6 designs (Figure 2), chosen by the Generation IV International Forum, with the objective to replace the previous generations and supply the demand for electricity and industrial applications in the future years using enhanced features, such as higher efficiency, reduction in waste production, economic competitiveness and improvement in proliferation resistance [3].

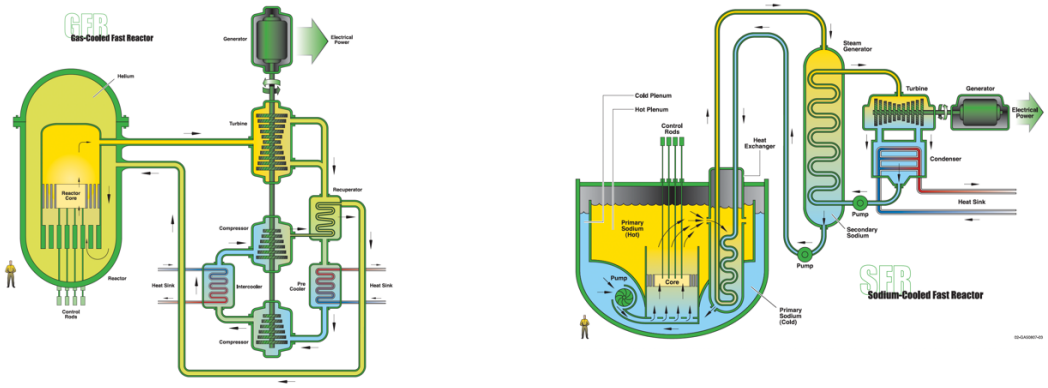

(a) Gas-Cooled Fast Reactor (b) Lead-Cooled Fast Reactor

Figure 2. Gen IV nuclear reactors. Reprinted from [3].

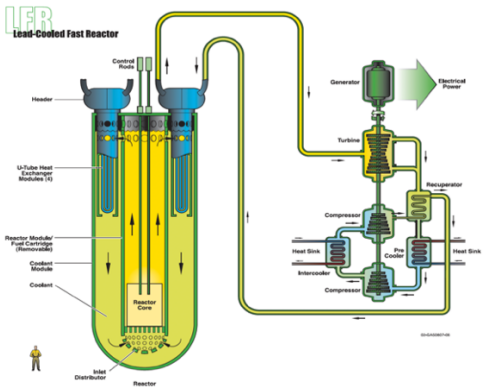

(c) Lead-Cooled Fast Reactor

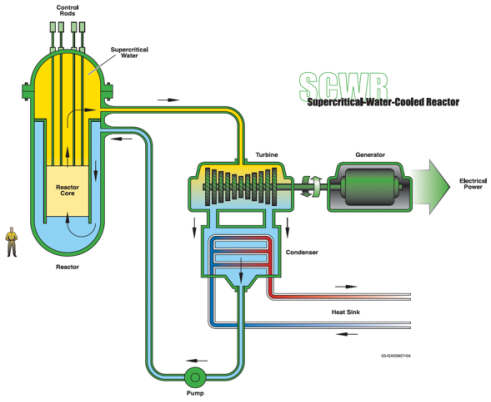

(d) Supercritical-Water-Cooled Reactor

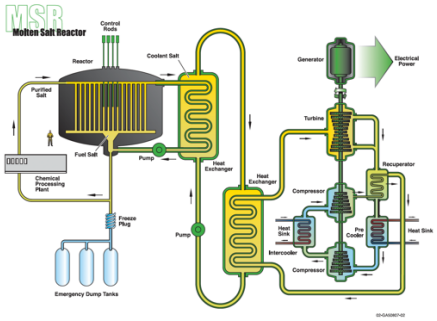

(e) Molten Salt Reactor

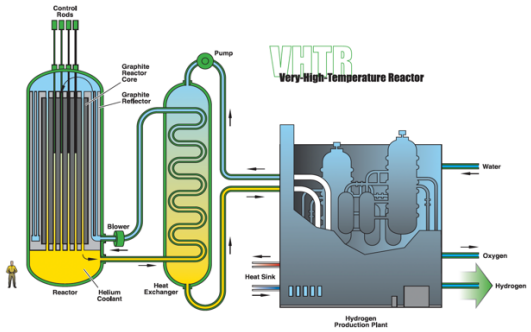

(f) Very-High Temperature Reactor

Figure 2. Continued.

Among the Gen IV designs, the Very High-Temperature Gas-Cooled Reactor (VHTR) has capabilities that, among others, improve the net electricity efficiency and provide process heat for a variety of application including efficient hydrogen production [4]. To maintain the reactor plant components in operational conditions and enhance safety levels in abnormal scenarios, the VHTR implements a passive Reactor Cavity Cooling System (RCCS) that removes heat leakage from the reactor cavity by means of natural circulation. This facility can use air or water as the cooling fluid [5] [6].

The present study focuses on a Water-cooled RCCS (WRCCS). Figure 3 shows a generic schematic of this design. The heat leakage from the reactor pressure vessel is transferred to the water running in the risers allocated in the cooling panels. The heated water, driven by natural circulation, goes up to a tank where it is cooled by the cold water inside. Then, the water returns to the risers through the downcomer, closing the natural circulation loop.

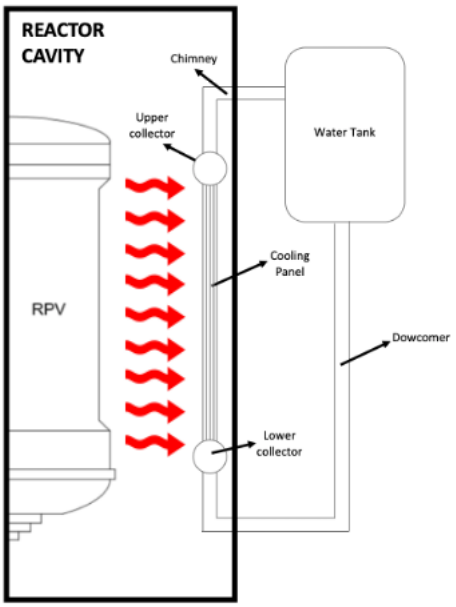

Figure 3. Water-cooled RCCS schematic design overview.

Natural circulation is used in several engineering applications besides the RCCS, such as cooling electronic circuits and air conditioning, among others, due to high reliability since it does not depend on any kind of external energy source. The functionality

principle is based on the difference in fluid density as it is heated. In the case of the RCCS, the heat primarily comes from irradiation and convection from the reactor vessel [7].

At Texas A&M University (TAMU), Vaghetto [8] designed and constructed a scaled WRCCS experimental facility to study its thermal-hydraulic behavior during steady-state and transient conditions, contributing to the development of the RCCS. Additionally, the detailed experimental data collected provides an opportunity to validate system thermal hydraulic codes and computer fluid dynamics (CFD) analysis. The facility consists of a primary loop comprising a portion of the reactor cavity (heaters and nine coolant risers), a hot and cold leg, and a tank (sink reservoir). There is also a secondary loop that maintains the temperature of the tank allowing the system to operate in a steady-state condition. The facility will be described in detail in the upcoming sections. Vaghetto [8] used RELAP5-3D to validate the scaling procedure. The results from the experiments proved the heat removal capabilities of the facility and helped to understand the thermal-hydraulic phenomena that can take place within it.

Quintanar [7] implemented updates in the TAMU WRCCS facility and investigated the flow and temperature distribution under steady-state conditions. It was found that within the range of *Re* analyzed, the temperature and flow distribution in the cooling risers are symmetric for the low *Re* cases and asymmetric for the high *Re* cases.

Holler [9] performed multiple analyses and experimentation with optic fiber distributed temperature sensors (OF-DTS) in both water and air environments. In the WRCCS, the author measured the temperature profile of the cooling risers with OF-DTS and compared

it with thermocouple measurements. A good agreement was found between both measurement techniques.

As previously mentioned, the WRCCS experimental facility also provides means of validating computational tools used to predict the various phenomena occurring within. Gorman et al [10] developed a CFD model of the WRCCS test section (cooling panel) using the ANSYS FLUENT. A simulation of the steady-state conditions was performed and compared against experimental temperature and velocity distributions, showing good agreement between them.

Pehlivan [11] used RELAP5/SCDAPSIM system code to model the WRCCS and simulate its behavior during normal and accidental scenarios. They found that the simulation results match the experimental data.

Following this thread, the present work aims to demonstrate the capability of Flownex Simulation Environment (SE) [12] to predict the thermal-hydraulic behavior of the TAMU WRCCS experimental facility. So far, there is no WRCCS simulation performed using Flownex SE. By doing so, the author seeks to contribute to bringing confidence and broadening the availability of options for similar analysis in the nuclear field.

Flownex is a solution for system and sub-system level simulation [13]. The software is able to analyze and optimize complete thermal-hydraulic and thermodynamic networks. It also includes tools for constraint design, sensitivity analysis of components and system parameters. The code can model a variety of applications, such as gas, steam or combined power plants, nuclear power plant, gas turbine combustion chambers, and

heat exchanger systems, among others. In the nuclear field, the extensive capabilities of Flownex merge into a tool that couples neutronics and thermal-hydraulic analyses. Other advantages of the software consist of fast processing, a friendly interface, and integration with engineering computational tools such as ANSYS, RELAP, and MCNP [14].

In the academic field, Rousseau et al [14] modeled an air-cooled RCSS with two different one-dimensional system codes, Flownex and Gamma+. They found good agreement between the results from both simulation environments if the same required input data is used, showing the ability of both software in solving the fundamental conservation and heat transfer relations for a complex system. Also, du Toit [15] investigated the effects of pipe diameter, loop length and local losses on steady-state single-phase natural circulation of water in square loops using Flownex.

Here, Flownex is used to model and simulate the TAMU WRCSS facility. Three representative steady-state operational conditions, defined by the bulk volumetric flow rate through the system, are simulated (Re = 2409, Re = 2490, and Re = 11524). The Flownex simulation results of the cavity outlet temperature, the temperature profile along each riser, and the volumetric flow rate split in the cooling panel, are compared with experimental data ([7], [9]) and previous RELAP simulations [11]. These parameters are important to characterize the facility's thermal-hydraulic behavior. The flow and temperature distributions permit us to assess the capability of heat removal of the RCCS and understand the response of the system for steady-state, accidental, and other transient scenarios.

Also, a sensitivity analysis assessing the impact on system's temperature and flow rate due to power reduction is conducted. Lastly, an accident scenario considering the loss of the secondary coolant of the facility is performed.

2. OBJECTIVES

Based on the experimental data acquired in the TAMU WRCCS as well as the simulations results obtained by previous studies, this thesis develops a model of the facility using Flownex and performs simulations for the steady-state and transient operational conditions, taking into account different system pressure drops in the loop (*Re* cases), in order to:

I. Compare and analyze the outlet temperature simulation result against experimental data.
II. Analyze the temperature distribution along the risers and compare results against the experimental data.
III. Analyze the volumetric flow rate split across the risers obtained from the Flownex simulation and compare against previous studies.
IV. Perform a sensitivity analysis by decreasing the power delivered to the risers.
V. Model a loss of the secondary coolant scenario.

To meet those goals, the following tasks are performed:

1. Understand the methodology, capabilities, and limitations of one-dimensional system codes.
2. Develop a model of the WRCCS experimental facility by using representative built-in components from the Flownex library.
3. Simulate the network for the steady-state condition applying the appropriate setup conditions used in the experiments for the *Re* cases.
4. Simulate a transient condition representing an accident scenario.

3. THE RCCS EXPERIMENTAL FACILITY

To accomplish the objectives of this thesis, a model of the scaled WRCCS experimental facility is developed using Flownex. This topic describes the facility including all its features along with an explanation regarding its operation.

3.1. Facility Description

The experimental facility modeled in Flownex is a 1:23 axial scaled water-cooled RCCS [7]. Figure 4 shows the main components of this installation.

The primary loop consists of a portion of a reactor cavity (heaters and the cooling panel with nine risers), hot and cold legs and a water tank. The electrical radiant heaters (6) increase the water temperature in the nine risers (1), which ultimately establishes natural circulation in the system due to buoyance forces. The heated water flows upward and is collected by the upper manifold (3). Then, it flows through the hot leg (7) where it reaches the water tank (4). In the water tank, heated water is cooled by mixing with cold water from the secondary loop.

Cooled water from the tank goes downwards through the cold leg (5), reaches the lower manifold (2) and is distributed among the risers. A valve placed in the tank outlet controls the pressure drop in the loop, which in turn defines the bulk volumetric flow rate measured by the flowmeter (8).

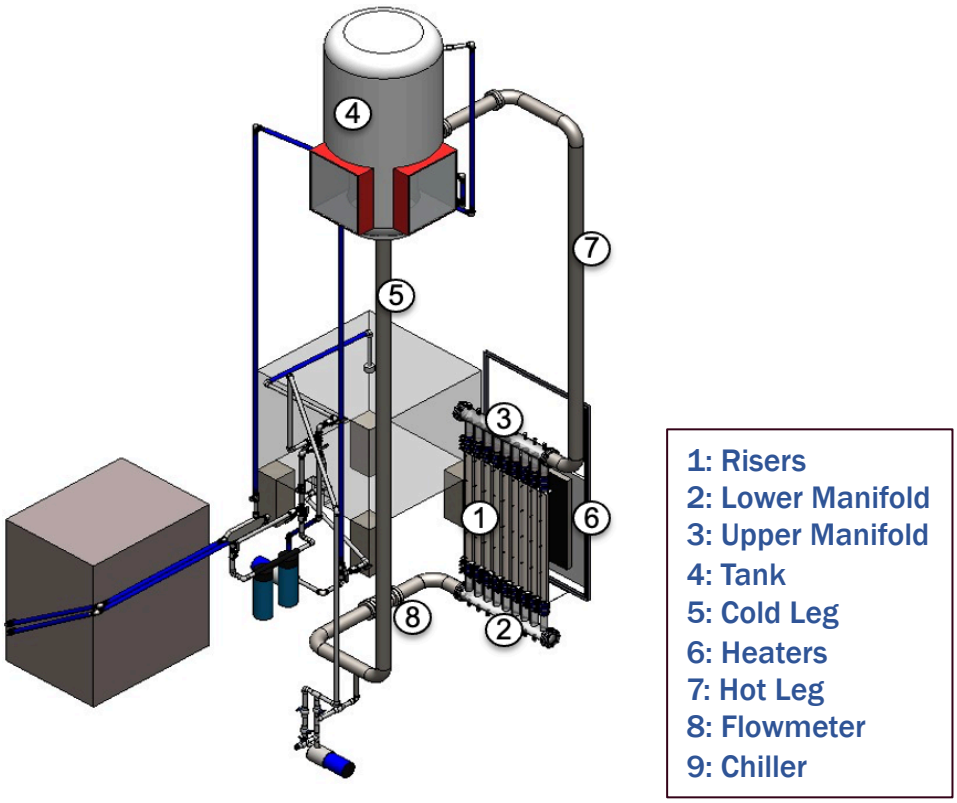

Figure 4. TAMU RCCS facility representation.

A secondary loop is responsible for maintaining a steady-state condition in the primary loop by removing heat from the water tank. Figure 5 shows a schematic of both loops. In the secondary loop, the water from the tank is circulated by a pump through a heat exchanger. The chiller ultimately removes heat to the ambient environment.

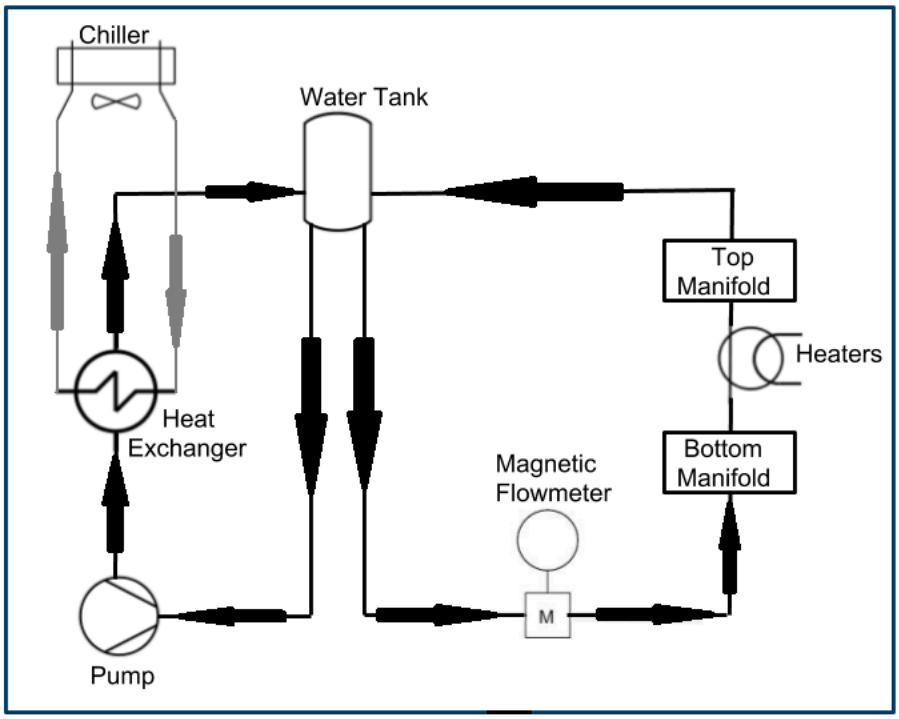

Figure 5. Primary and secondary loops. Reprinted with permission from [16].

3.2. WRCCS Experimental Data

The main experimental data used for comparison against the simulation comes from the facility test section presented in Figure 6. The test section consists of the nine risers (1), the lower (2) and upper (3) manifolds, and the reactor cavity inlet and outlet pipes. To collect the experimental data in the test section, there is a flowmeter (8), a set of five thermocouples at different levels of each riser (uncertainty of ± 1.1ºC), and Resistance Temperature Detector (RTD) sensors at the inlet and outlet pipes (uncertainty of ± 0.2ºC). The manifolds are made of transparent material so that flow visualization through Particle Image Velocimeter (PIV) techniques can be used.

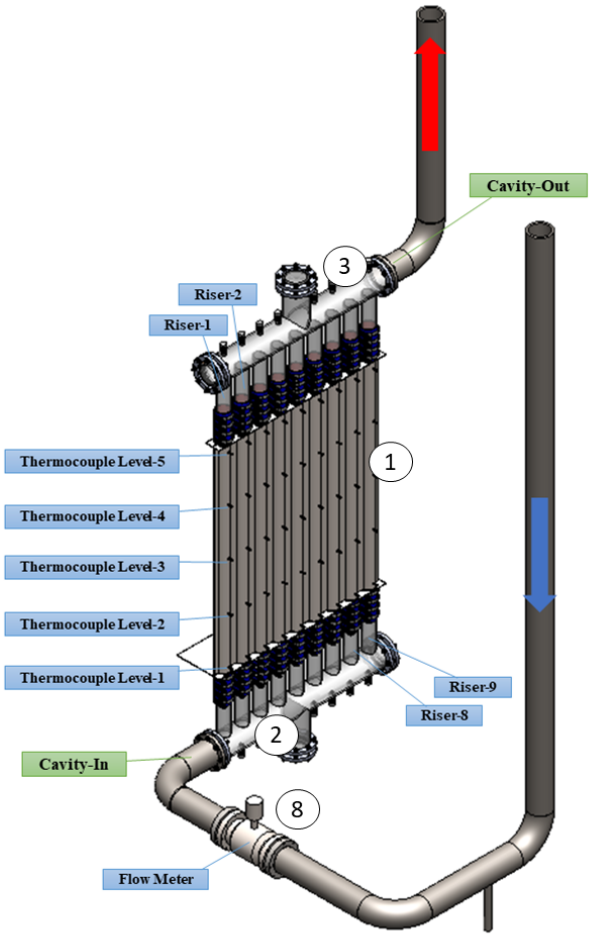

Figure 6. WRCCS test section representation.

In this thesis two main data sets (comprising temperature and flow rate measurements) are compared with the simulation results. The first data set was acquired by the experiments performed by Quintanar [7] (named Data Set 1) and the second one was acquired by Holler [9] (Data Set 2). For the second data set, the volumetric flow rate split across the risers is compared against the RELAP simulation results obtained by Pehlivan [11]. Each data set has one or two cases consisting of different *Re* defined by a

given pressure drop in the loop controlled by the valve opening. Table 1 summarizes the cases that the WRCCS is simulated in Flownex.

Table 1. Simulation cases.

Data Set	Case (*Re*)	Valve Opening (%)	Bulk Volumetric Flow Rate
1	2490	25	9.6
2	2409	25	8.2
	11524	100	39.0

3.2.1. Data Set 1

Quintanar [7] ran the experimental facility for four different steady-state operational conditions; each one representing a bulk volumetric flow rate through the system (valve opening of 25%, 50%, 75%, and 100%). His focus was on acquiring the velocity profile in the lower manifold with PIV techniques. He observed that the last three conditions have the same behavior regarding temperature readings in the thermocouples and flow profile in the test section.

The main experimental parameters for the valve opening of 25% (*Re* = 2,490 case) is presented in Table 2. This case is used to be compared with the Flownex simulations.

The temperature of the water in all thermocouples levels in each riser are indicated in Figure 7 for the *Re* = 2,490 case.

Table 2. Data Set 1: main experimental parameters for WRCSS test section.

Parameters	**Operational condition**
Valve Opening Case (%)	25
Reynolds Number	2,490
Primary Loop Volumetric Flow Rate (lpm)	9.6 ± 0.3
Water Inlet Temperature to Lower Manifold - Cavity In (°C)	30.4 ± 1.1[a]
Water Outlet Temperature from the Upper Manifold - Cavity Out (°C)	40.0 ± 1.1[a]
Net Power (W)	6000

Note:
[a] The cavity-in and cavity-out temperatures were measured with thermocouples for this data set.

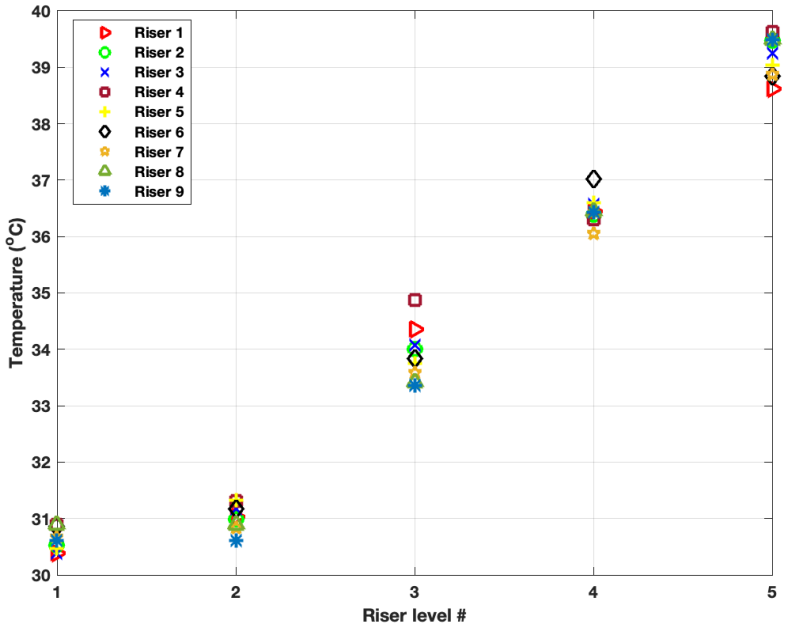

Figure 7. Risers' experimental temperature profile for Data Set 1.

The volumetric flow rate split across the risers is calculated according to the relationship below based on the velocity profiles acquired in each branch of the manifold [7] :

$$\dot{v}\left[\frac{l}{min}\right] = U\ \left[\frac{m}{s}\right] \cdot A[m^2] = \ R \cdot U_{bulk}\left[\frac{m}{s}\right] \cdot \frac{\pi \cdot D^2[m^2]}{4} \cdot \frac{1000[l]}{\frac{1}{60} min} \tag{1}$$

$$\dot{v} = R \cdot U_{bulk} \cdot \frac{\pi \cdot D^2}{4} \cdot 60000 \tag{2}$$

Where,

- $\dot{v}$ – volumetric flow rate in each riser
- A – cross area of the risers
- D – diameter of the risers
- R – non-dimensionalized flow velocity parameter acquired in the experiment [7]
- U – flow velocity in each riser
- U_{bulk} – bulk flow velocity of the loop acquired in the experiment [7]

The calculated volumetric flow rates along with the related parameters are shown in Table 3. The bulk velocity flow is U_{bulk}= 19.0 mm/s and D = 52.5 mm [7].

Table 3. Estimated volumetric flow rate across the risers based on the non-dimensionalized velocity profile (R).

R	V (m/s)	$\dot{v}$ (l/min)
0.4443	0.0086	1.0439
0.4707	0.0091	1.1059
0.4929	0.0095	1.1581
0.5148	0.0099	1.2095
0.4650	0.0090	1.0925
0.4442	0.0086	1.0436
0.3688	0.0071	0.8665
0.5133	0.0099	1.2060
0.4255	0.0082	0.9997

3.2.2. Data Set 2

Holler [9] acquired the experimental data in the WRCSS for the representatives low and high *Re* cases (valve opening of 25% and 100%). Table 1 shows the main experimental parameters for those cases. The Secondary Tank Inlet Temperature is the temperature measured between the heat exchange and the tank (see Figure 5).

Table 4. Data Set 2: main experimental parameters for WRCSS test section.

Parameters	**Operational condition**	
Valve Opening Case (%)	25	100
Reynolds Number	2,409	11,524
Secondary Tank Inlet Temperature (°C)	30.8± 1.1	30.8± 1.1
Primary Loop Volumetric Flow Rate (lpm)	8.2 ± 0.3	39.0 ± 0.6
Water Inlet Temperature to Lower Manifold - Cavity In (°C)	35.8 ± 0.2[a]	36.1 ± 0.2[a]
Water Outlet Temperature from the Upper Manifold - Cavity Out (°C)	48.4 ± 0.2[a]	38.9 ± 0.2[a]
Net Power (W)	7,153 ± 290[b]	7,555 ± 550[b]

Note:
[a] The cavity-in and cavity-out temperatures were measured with RTD sensors for this data set.
[b] Estimated error of the power [17].

The temperature of the water in all thermocouples levels in each riser are indicated in Figure 8 for both *Re* cases.

Pehlivan [11] used Data Set 2 to compare the RELAP simulations results against the experimental data of the WRCCS facility. Here, the Flownex prediction for the flow rate split across the risers is compared against the RELAP result [11] for Data Set 2 (Table 5).

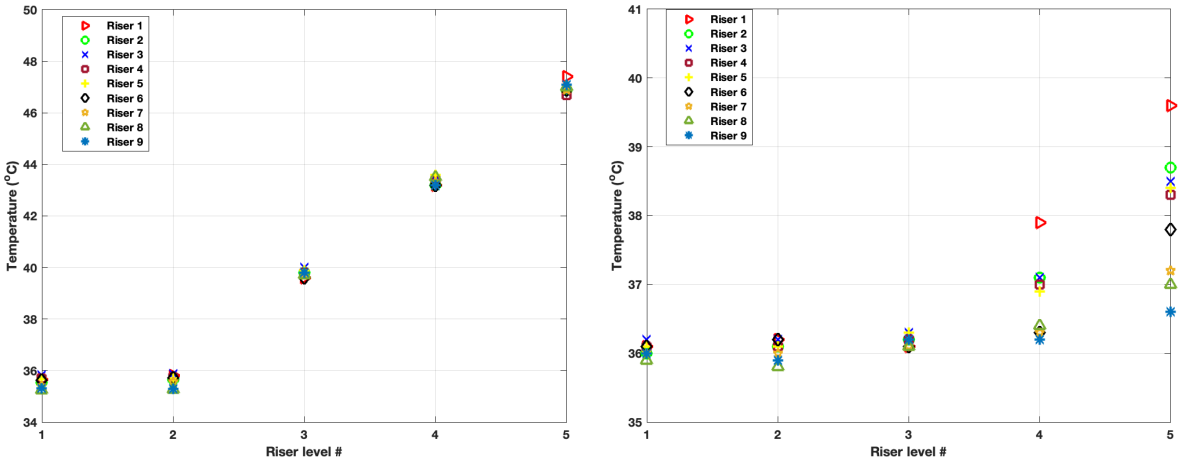

(a) *Re* = 2,409 (b) *Re* = 11,524

Figure 8. Risers' experimental temperature profile for Data Set 2.

Table 5. RELAP volumetric flow rate prediction.

Case / Riser	Flow Rate (lpm)	
	***Re* = 2409**	***Re* = 11524**
1	0.934	3.900
2	0.896	3.799
3	0.949	3.981
4	0.912	3.966
5	0.953	4.226
6	0.888	4.270
7	0.880	4.550
8	0.875	4.938
9	0.864	5.428

4. FLOWNEX RCCS MODEL

Flownex is a system-level one-dimensional thermal-fluid code. 1D codes are often used to model entire networks where CFD simulation would be computationally expensive. It allows quick evaluation of "what if scenario" by simulating small changes in design and system parameters. One of the main drawbacks of this kind of system-level codes is the lack of detailed analysis [18].

Application of 1D and 3D codes can be presented in terms of a manufacturing "V" diagram (Figure 9). Generally, 1D is used on the top portion and 3D analysis is carried out as more accurate evaluation is required.

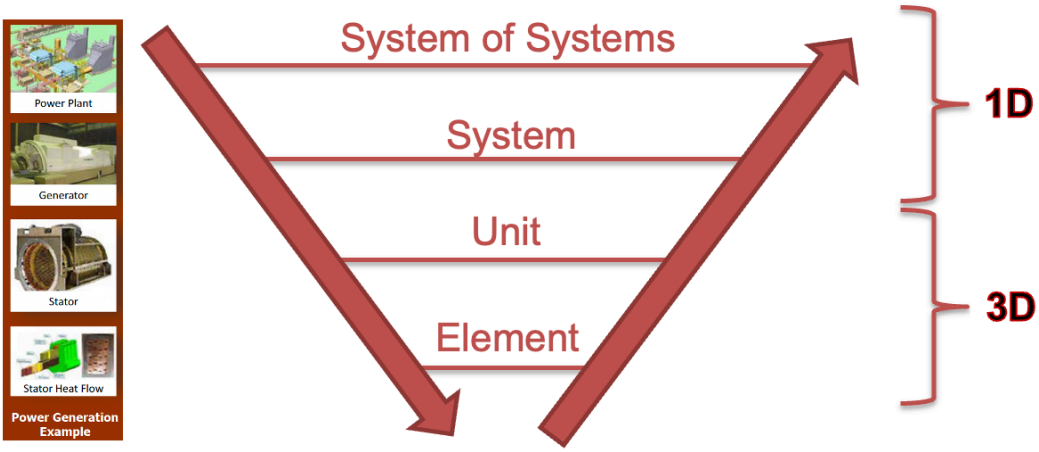

Figure 9. "V" diagram and simulation level analysis.

Flownex is based on an implicit pressure correction solution method [19] and it solves the steady-state and transient forms of the fundamental conservation equations of fluid dynamics and heat transfer [20].

The one-dimensional form of the continuity equation is given by:

$$\frac{\partial \rho}{\partial t} + \frac{\partial (\rho V)}{\partial x} = 0 \tag{3}$$

Where ρ is fluid density, t is time, x is the direction of the flow and V is the velocity. Eq. (3) states that mass in a differential control volume varies in time if there is mass entering or exiting this control volume.

The momentum equation for one direction is given by:

$$\frac{\partial (\rho V)}{\partial t} + \frac{\partial (\rho V^2)}{\partial x} = -\frac{\partial p}{\partial x} - \frac{f \rho |V| V}{2D} - \rho g \frac{\partial z}{\partial x} \tag{4}$$

Where f is the Darcy-Weisbach friction factor, D is the hydraulic diameter and g is the gravity.

The left-hand side of Eq. (4) represents the inertial terms, composed of a time derivative and convective contributions. The right-hand describes the forces acting on the differential control volume. The pressure gradient and the Darcy-Weisbach formula represent the surface forces while the remaining term is the body force, which in this case, it is due to the gravity.

Finally, the energy conservation equation, expressed as a function of the specific stagnation enthalpy h_o, is given by:

$$\frac{\partial(\rho(h_o + gz) - p)}{\partial t} + \frac{\partial\big(\rho V(h_o + gz)\big)}{\partial x} = \dot{Q}_h - \dot{W} \tag{5}$$

Where z is the height, $\dot{Q}_h$ is the heat provided to the control volume and $\dot{W}$ is the work done on the environment. The specific stagnation enthalpy is defined as:

$$h_o = h + \frac{V^2}{2} \tag{6}$$

Where h is the specific enthalpy given in function of the u specific internal energy, pressure p and specific volume v:

$$h = u + pv \tag{7}$$

The Flownex solution also uses built-in thermal-hydraulic relations and properties along with a pre-configured library of components to give information at any point of the system about temperature, pressure, mass flow rate, power, and heat transfer [14].

The component library provides a variety of options that are added to a canvas to form complex networks. Common components include pipes, connections, valves, heat exchangers, pumps, and turbines. These components are linked through nodes, tanks, or

reservoirs (linking items). The linking items connect the inlet and outlet of the component where boundary conditions can also be set. Figure 10 shows a schematic network formed by components and nodes in Flownex.

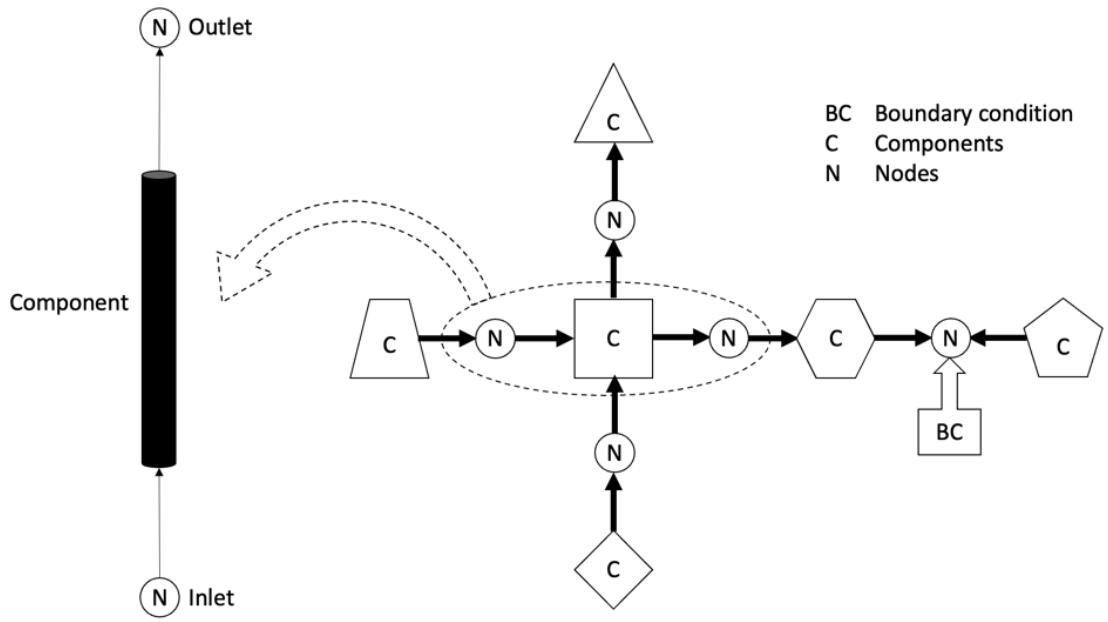

Figure 10. Flownex schematic network.

The implicit pressure correction solution method algorithm [19] used in Flownex follows the steps described in Figure 11 [20].

The component's parameter results are a weighted average value between its inlet and outlet [14]. Discretization of specific components can be made so that higher accuracy is achieved. For instance, a single pipe can be subdivided (discretized) and the parameter result values are weight-averaged through all increment nodes created.

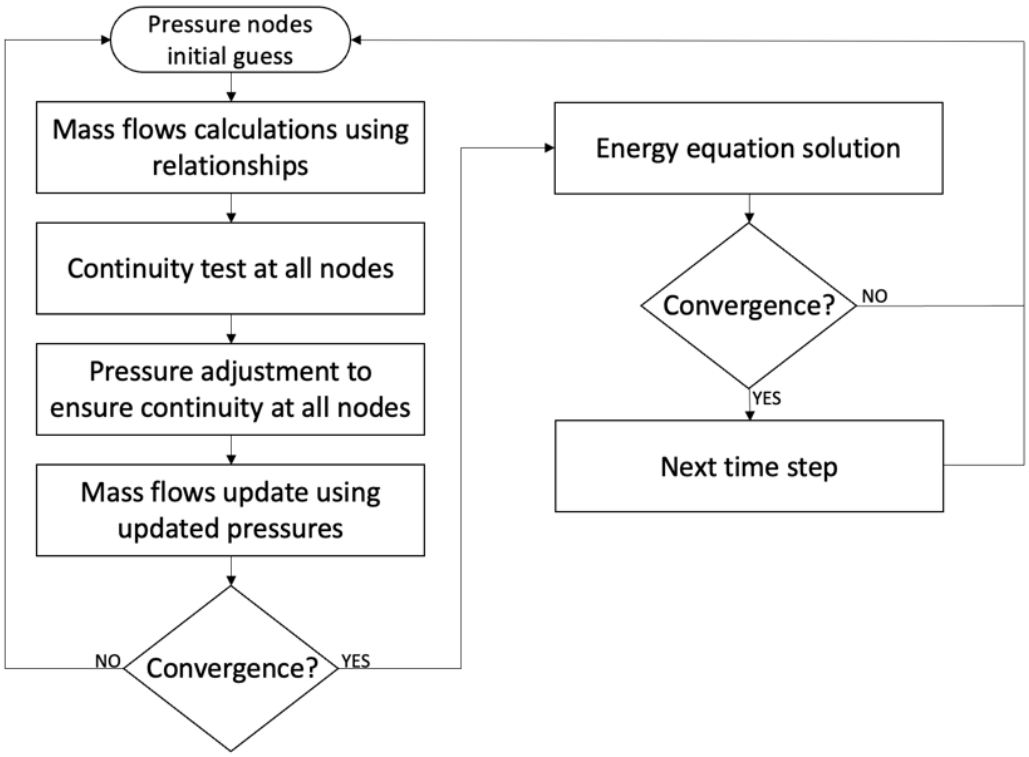

Figure 11. Flownex solution method.

Figure 12 shows the Flownex network model for the WRCSS facility under study. The primary loop is modeled with an open container component (tank), a valve, pipes to form the cold and hot legs, and "T" connections and pipes for the cooling panel (risers, lower and upper manifolds). The secondary loop consists of a set of pipes. The chiller (heat sink) is modeled as a pipe with a fixed exit temperature (T_{sink}).

The model uses two input data in the secondary loop, the secondary tank inlet temperature (T_{sink}) and the secondary volumetric flow rate ($\dot{v}_2$). T_{sink} indicates the water temperature measured in the tank inlet at the secondary loop side, according to the value

from Table 4 (for Data Set 1, this value was not recorded). The value of $\dot{v}_2$ was adjusted so that the predicted cavity inlet temperature (T_{in}) matches the experimental one. For the primary loop inputs, atmospheric pressure (P_{atm}) was set in the tank free surface and the heat (Q_{add}) provided to the cooling panel, shown as Net Power in Table 2 and Table 4, was axially distributed in each riser based on a parabolic approximation of the model used in [11].

The pressure drop in the WRCCS model was set to match the bulk volumetric flow rate for each case by adjusting the secondary losses in the system. After losses for bends and junctions were applied, an adjustable valve component was used for the final tuning.

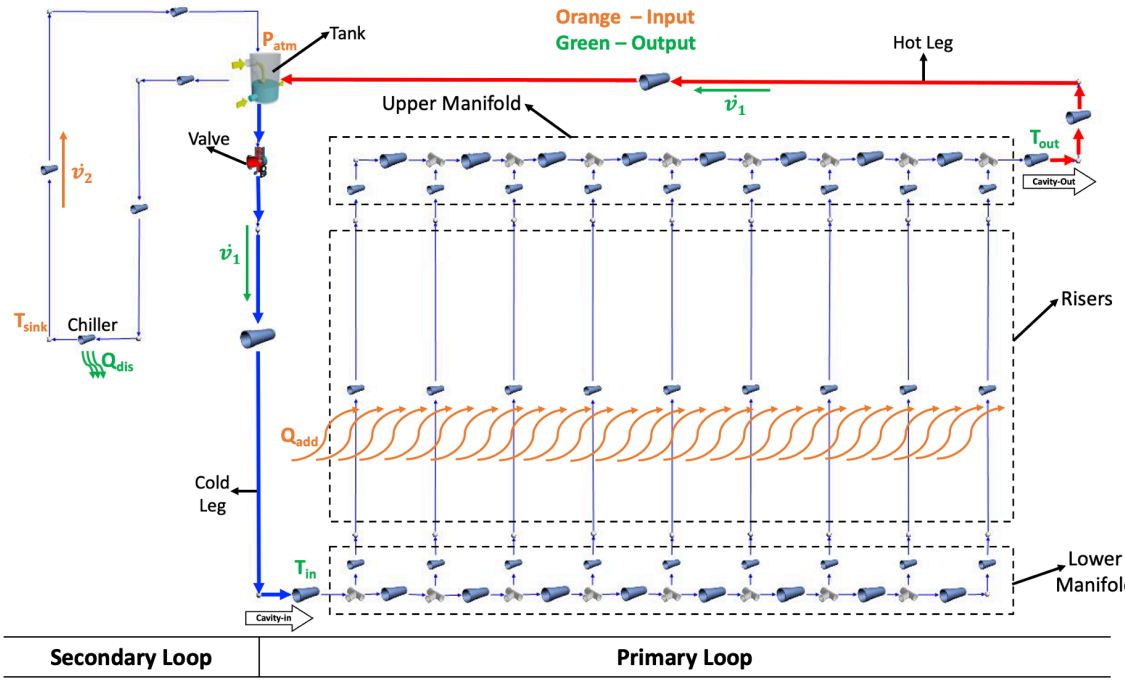

Figure 12. WRCCS Flownex model.

5. RESULTS AND DISCUSSION

This section presents the comparison of the simulation results against Data Set 1 and 2 for the cavity outlet temperature, risers' temperature profile, and flow rate split in the cooling panel. Later in this section, power reduction sensitivity analysis and loss of the secondary coolant scenario are simulated in Flownex for Data Set 2 (Re = 2,409 case).

5.1. Flownex Simulation Results Comparison Against Data Set 1

Table 6 shows the input parameters for the WRCSS model and the main simulation results. Since there is no recorded data regarding the parameters of the secondary loop for this data set, $\dot{v}_2$ and T_{sink} are adjusted so that T_{in} matches the experimental value. Also, $\dot{v}_1$ is achieved by setting the pressure drop through the valve opening in Flownex to 23.5%.

Table 6. Input parameters and main simulation results for Data Set 1 (Re = 2,490).

Re = 2490 case			Data Set 1	Flownex
Input	2nd Loop Volumetric Flow Rate (lpm)	$\dot{v}_2$	-[a]	30.1
	Secondary Tank Inlet Temperature (°C)	T_{sink}	-[a]	28.0
	Net Power (W)	Q_{add}	6000	6000
Result	1st Loop Volumetric Flow Rate (lpm)	$\dot{v}_1$	9.6 ± 0.3	9.4
	Cavity In (°C)	T_{in}	30.5 ± 1.1	30.9
	Cavity Out (°C)	T_{out}	40.0 ± 1.1	40.0

Note:
[a] Not recorded in the experiment.

The Flownex prediction for cavity outlet temperature is in good agreement with the experimental measurements. The difference between these values is within the uncertainty of the equipment. In an evaluation of system-level code capabilities, this result has a paramount importance since they represent the energy balance solution of the entire network for a correspondent bulk volumetric flow rate.

The temperature results are presented in three approaches. Firstly, all temperature results are plotted so that the reader can learn the global behavior of the risers' temperature profile in the cooling panel. Secondly, a plot condensing the temperature differences between simulation and experimental values are shown. Finally, the Flownex temperature predictions are compared against the thermocouple readings level by level in the risers.

Figure 13 shows the Flownex predicted temperature results for all risers in every level.

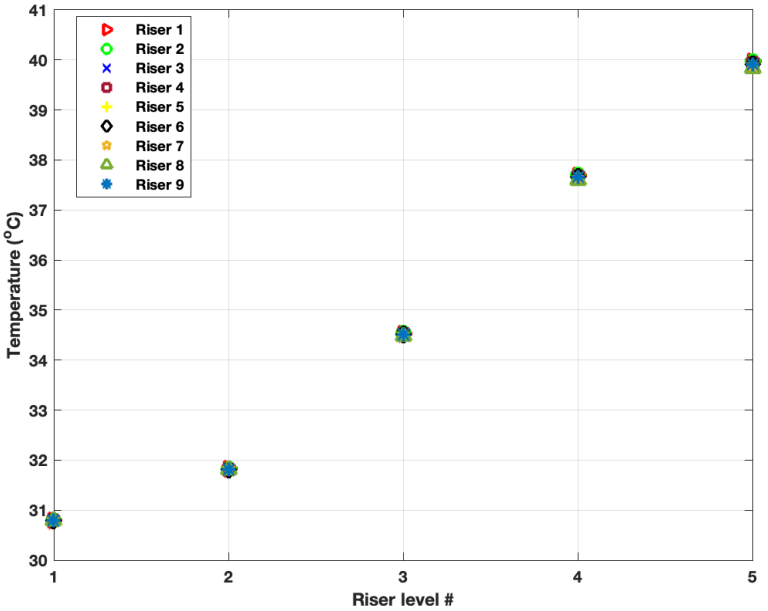

Figure 13. Risers' predicted temperature profiles (*Re* = 2,490).

Comparing the data in Figure 7 against Figure 13, we can see that the Flownex risers' predicted temperature profiles follow the same trend as the experiment. This is supported by the data in Figure 14 showing the risers' temperature difference between the Flownex prediction and experimental measurement are within the uncertainty of the equipment (±1.1°C) for 78% of the points.

The temperature difference is mostly higher than 1.1°C for the thermocouples located at level 4 of the risers. This may be due to the heat transfer profile input to the risers. The heat profile developed in [11] is an approximation of the heat flux imposed on the experiment (parabolic).

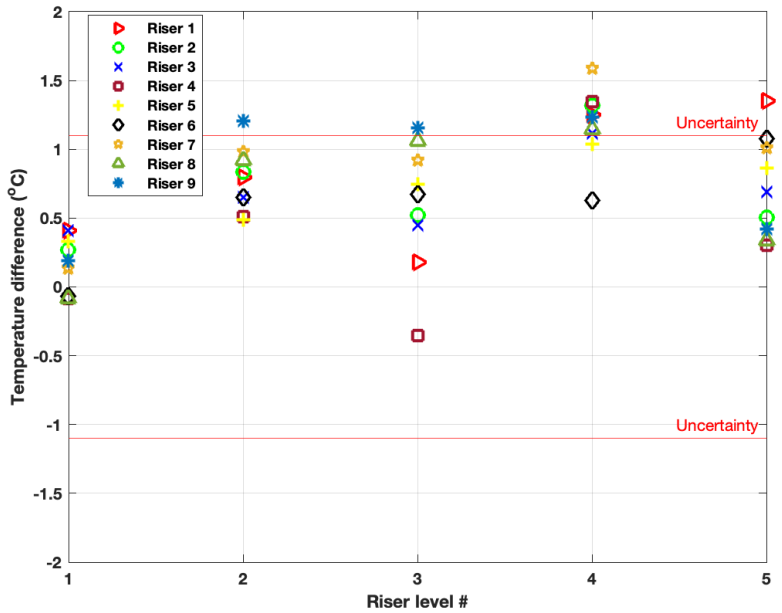

Figure 14. Temperature difference between thermocouple readings and simulation results for *Re* = 2,490 (thermocouple uncertainty is ±1.1°C)

Another approach to compare the experimental and predicted temperature values are given in Figure 15. The comparisons are carried out level by level to assess the behavior of the temperature distribution in each level as the heated water goes up through the riser.

For this case (*Re* = 2,409), the temperature distribution is similar at each level for all risers, as observed by [7] and [9]. In other words, the temperature has the approximately the same value at a given level across all risers.

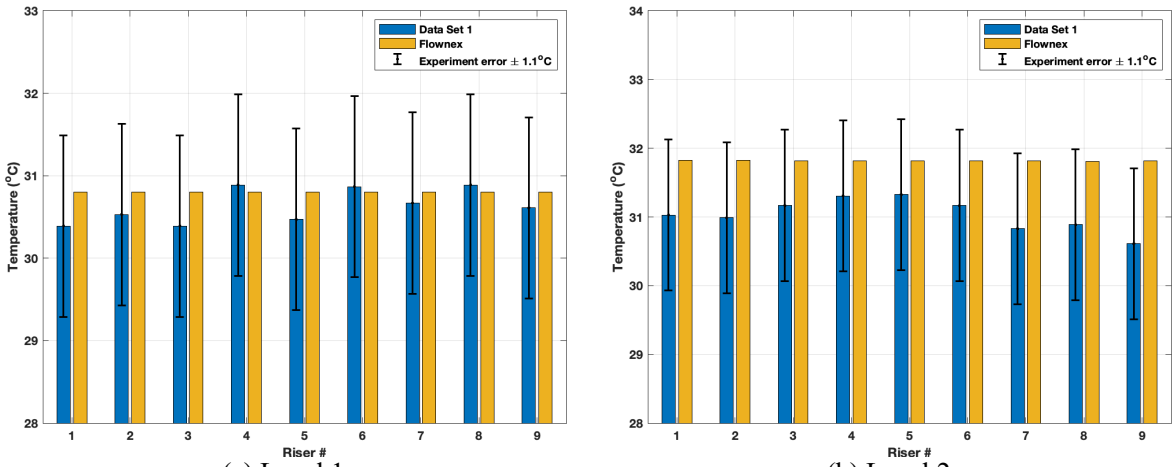

(a) Level 1 (b) Level 2

Figure 15. Risers' temperature comparisons by levels for *Re* = 2,490.

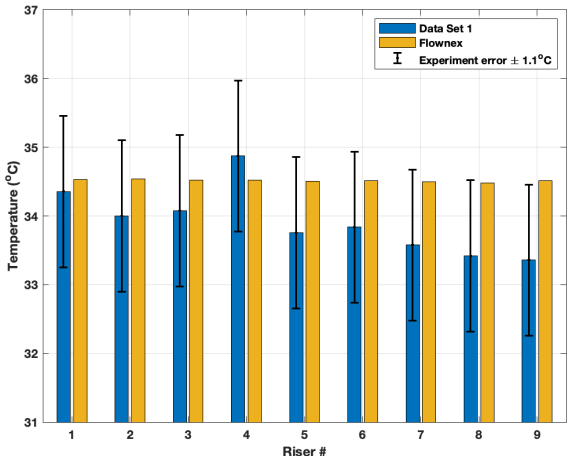

(c) Level 3

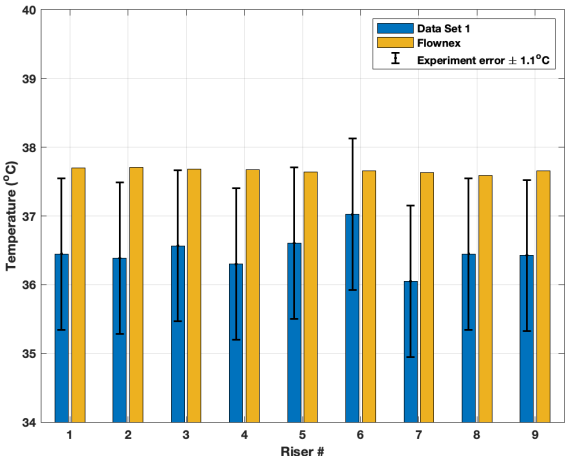

(d) Level 4

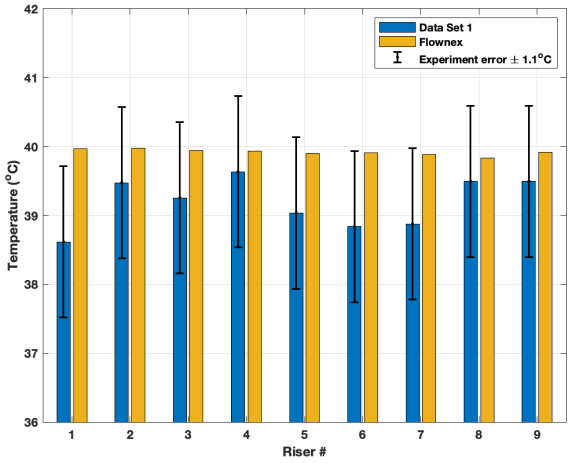

(e) Level 5

Figure 15. Continued.

The last parameter to be analyzed is the volumetric flow rate split among the risers. Figure 16 compares the Flownex results with the values from Table 3.

The distribution behavior of the flow is uniform across the risers, as observed by [7] and [9]. This result is expected since the temperature has the same uniform distribution for the *Re* = 2,490 case.

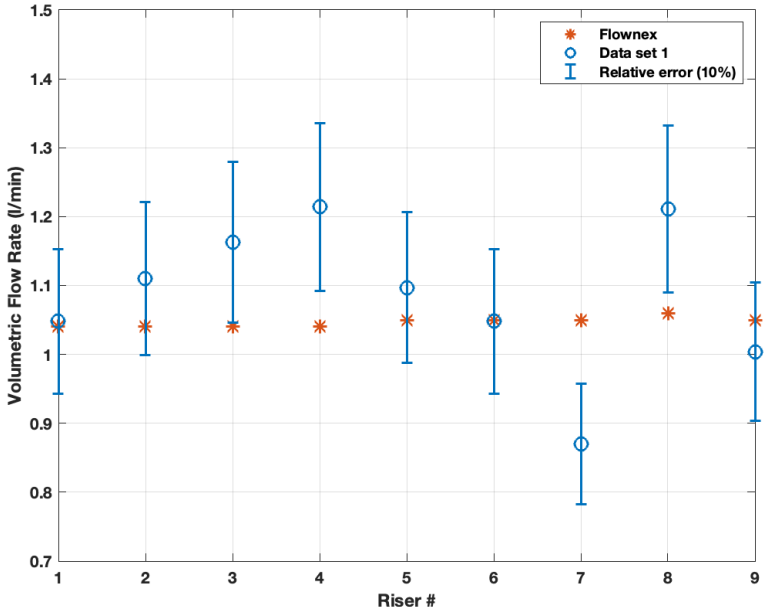

Figure 16. Volumetric flow rate split in the cooling panel for Flownex and experimental results (*Re* = 2,490).

The relative error is higher due to several factors related to the calculation of the experimental value presented in 3.2.1. The PIV technique does not account for the real physical phenomena, such as 3D velocity profiles. Also, the technique was applied in the branches of the manifolds, which does not represent faithfully the average velocity profile of the entire riser. However, considering these limitations and an error of 10%, it is seen from Figure 16 a reasonable agreement for more than half of the points.

5.2. Flownex Simulation Results Comparison Against Data Set 2

Table 7 shows the input parameters for the WRCSS model and the main simulation results for this data set. The $\dot{v}_2$ is adjusted so that T_{in} matches the experimental value. The valve opening is set in Flownex in 15% for *Re* = 2,409 and 100% for *Re* = 11,524.

Table 7. Input parameters and main simulation results for Data Set 2 (*Re* = 2,409 and *Re* = 11,524).

Case	Reynolds Number	*Re*	2,409		11,524	
			Data Set 2	Flownex	Data Set 2	Flownex
Input	2nd Loop Volumetric Flow Rate (lpm)	$\dot{v}_2$	-[a]	21.1	-[a]	21.1
	Secondary Tank Inlet Temperature (°C)	T_{sink}	30.8±1.1	30.8	30.8±1.1	30.8
	Net Power (W)	Q_{add}	7,153±290	7,100	7,555±550	7,500
Result	1st Loop Volumetric Flow Rate (lpm)	$\dot{v}_1$	8.2 ± 0.3	8.1	39.0 ± 0.6	39.4
	Cavity In (°C)	T_{in}	35.8 ± 0.2	35.6	36.1 ± 0.2	35.9
	Cavity Out (°C)	T_{out}	48.4 ± 0.2	48.3	38.9 ± 0.2	38.7

Note:
[a] Not recorded in the experiment.

Here again, the Flownex predictions for the cavity outlet temperatures are in good agreement with the experimental measurements. The differences between these values are also within the uncertainty of the equipment.

The temperature comparisons are performed as done for Data Set 1. The trends for the temperate distribution from both cases follow the experimental observation (Figure 8) as indicated in Figure 17.

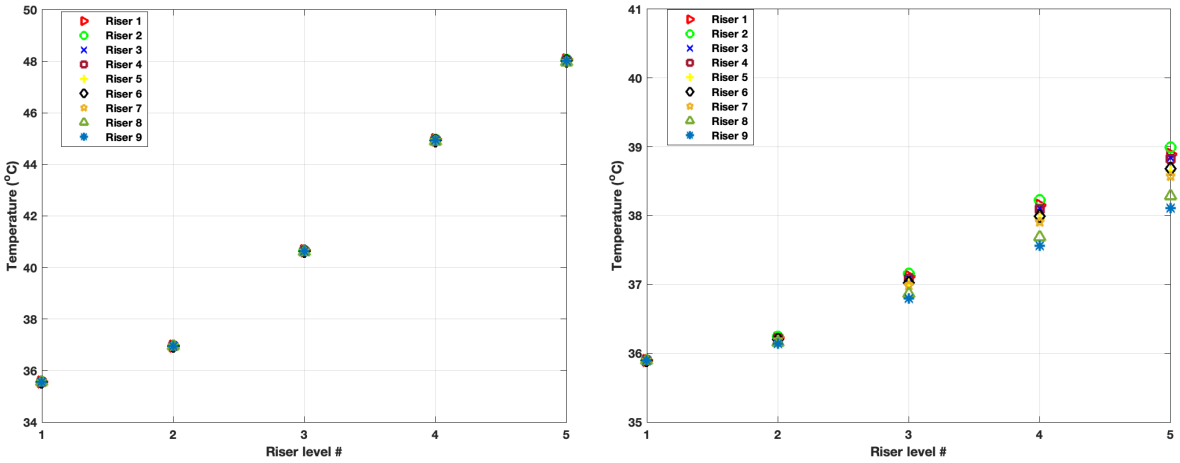

(a) *Re* = 2,409 (b) *Re* = 11,524

Figure 17. Risers' predicted temperature profiles for *Re* = 2,409 and *Re* = 11,524.

Figure 18 also supports the reasonable agreement regarding the experimental profile and the predicted one. Considering both cases, 70% of the comparisons are within the uncertainty of the equipment. The higher temperature differences, considering the uncertainty of 1.1°C, are located at level 4 of the risers in both cases, as occurred in Data Set 1.

Additionally, the higher heat added to the cooling panel for this data set compared to Data Set 1 along with the increased heat transfer related to low flow rate highlight a lower prediction's accuracy at level 2 as shown in Figure 18-(a). From Figure 8-(a), the experimental water temperatures at levels 1 and 2 are similar, which suggests that heat in the experiment may not be sufficiently transferred to this portion of the risers.

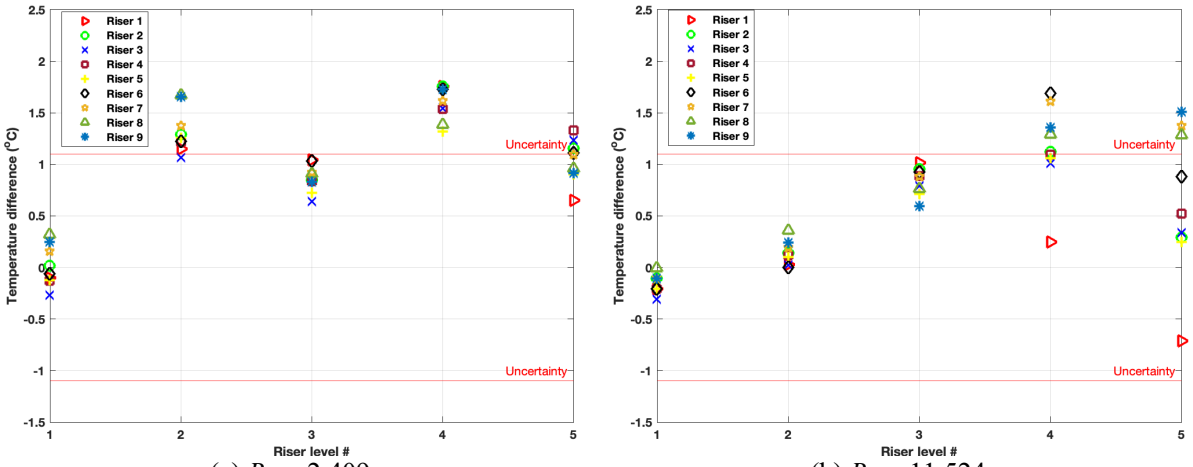

(a) Re = 2,409 (b) Re = 11,524

Figure 18. Temperature difference between thermocouple readings and simulation results for Re = 2,409 and Re = 11,525 (thermocouple uncertainty is ±1.1°C)

The comparisons of the risers' temperature in every level are carried out in Figure 19. For the lower Re, the distribution is the same as the one shown for Data Set 1. The temperature at a given level has the same value across all risers.

However, for Re = 11,524, as the water increases its temperature while it goes up in the risers (reaching levels 4 and 5, Figure 19), the distribution of the temperature across the risers becomes non-uniform with a decreasing trend as the riser position moves away from the cavity inlet pipe (Figure 6).

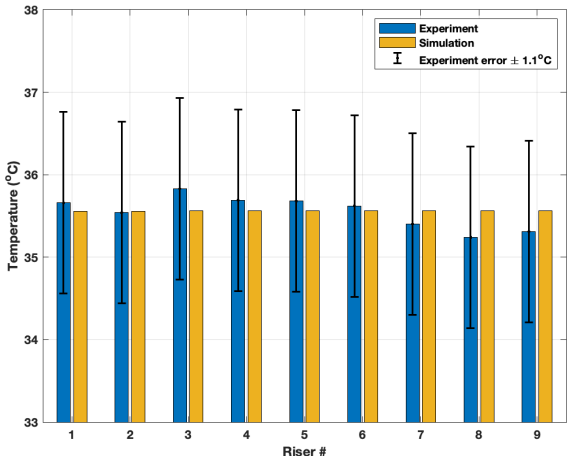

(a1) Level 1 – *Re* = 2,409

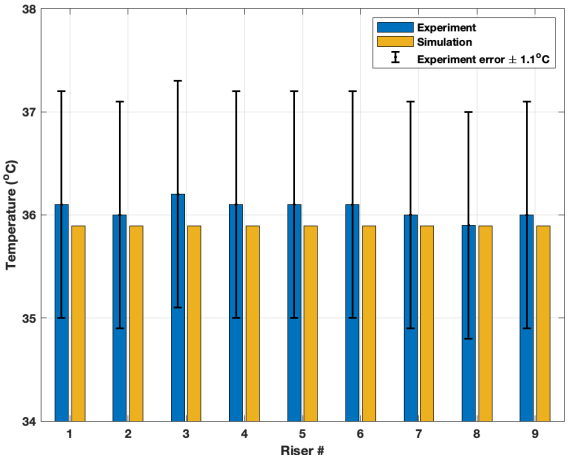

(b1) Level 1 – *Re* = 11,524

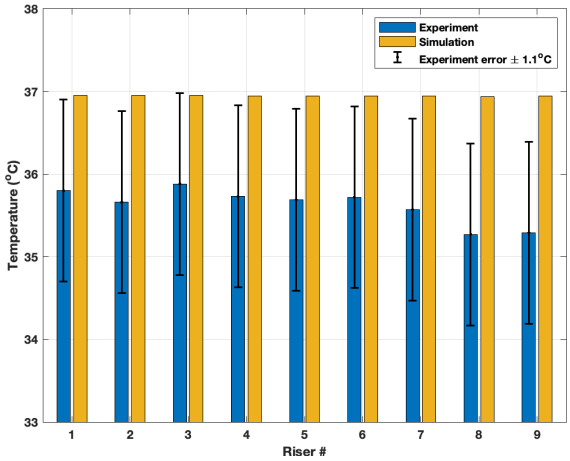

(a2) Level 2 – *Re* = 2,409

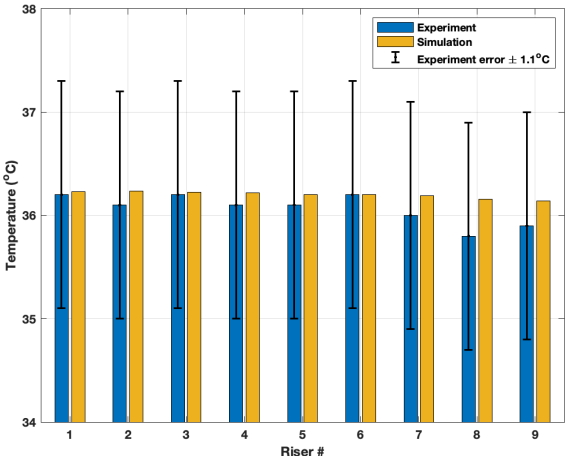

(b2) Level 2 – *Re* = 11,524

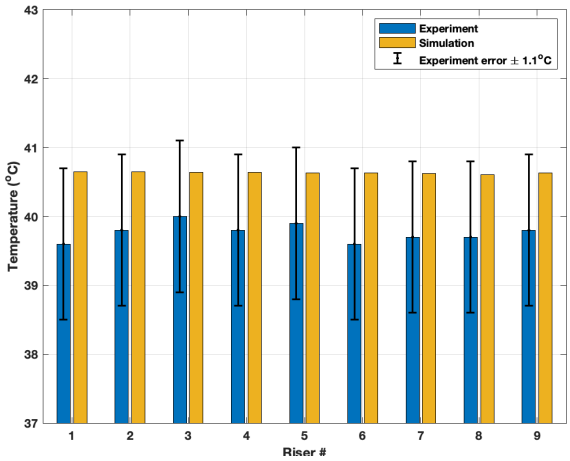

(a3) Level 3 – *Re* = 2,409

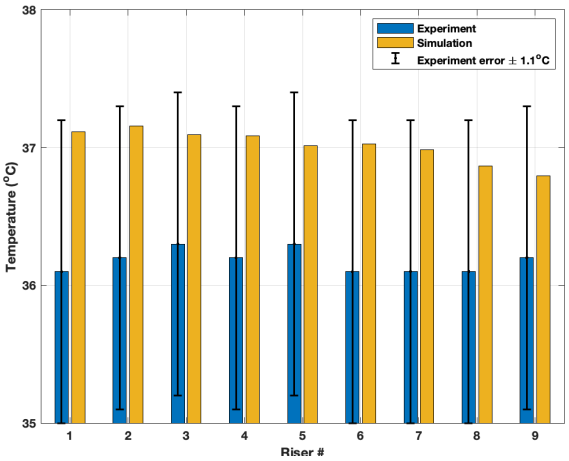

(b3) Level 3 – *Re* = 11,524

Figure 19. Risers' temperature comparisons by levels (*Re* = 2,409 and *Re* = 11,524).

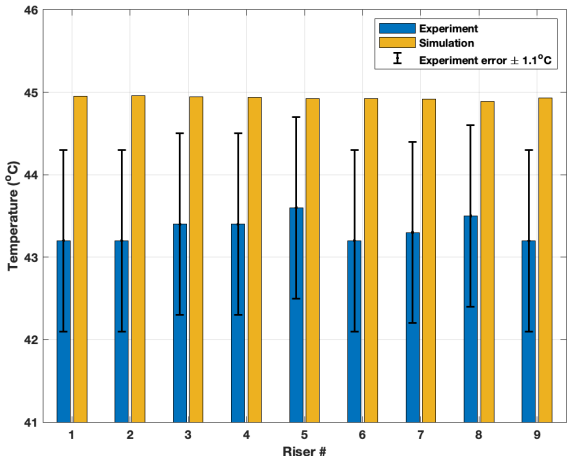

(a4) Level 4 – *Re* = 2,409

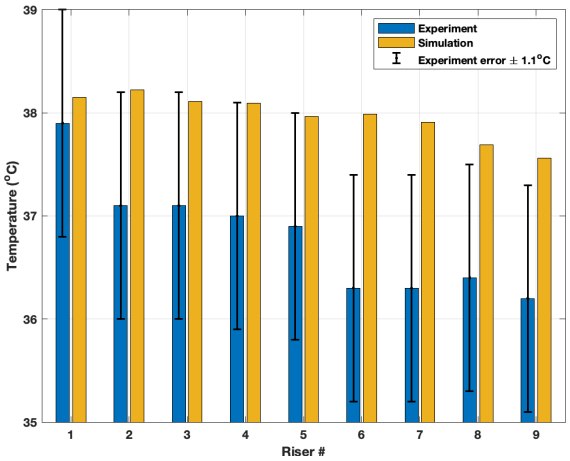

(b4) Level 4 – *Re* = 11,524

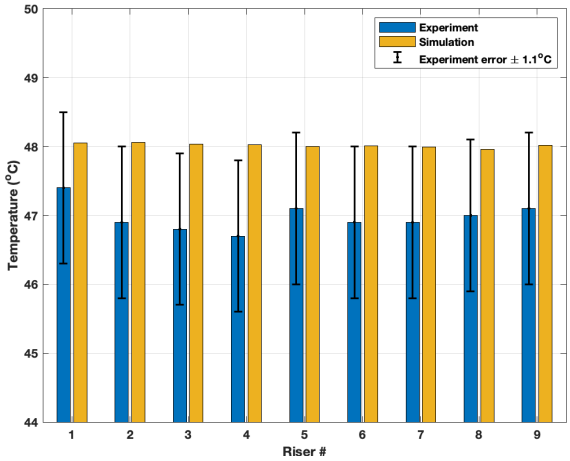

(a5) Level 5 – *Re* = 2,409

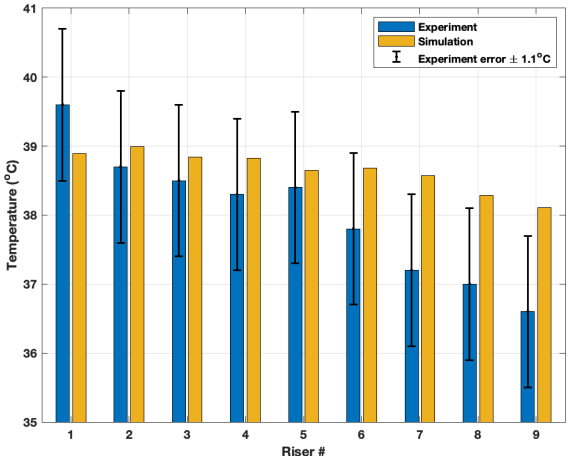

(b5) Level 5 – *Re* = 11,524

Figure 19. Continued.

A compatible trend with the temperature distribution across the risers is observed in the flow split (Figure 20). For the lower *Re* case, the volumetric flow rate is evenly divided. For the higher one, the volumetric flow rate increases as the riser moves away from the inlet pipe. These results are in accordance with the experimental observations [8] [9].

The comparisons of the Flownex predictions are made against the RELAP [11] for this data set. The error bar of 5% represents the relative error between the simulation results (considered an acceptable value for the code simulation comparison under study). The average relative error between both simulation results is 3% for the low *Re* case and 2% for the high one.

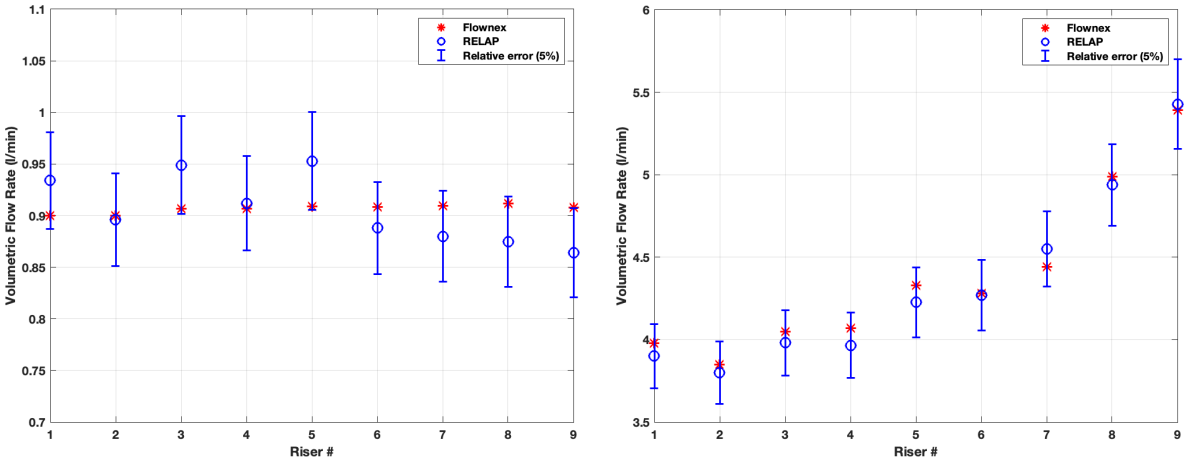

(a) *Re* = 2,409 (b) *Re* = 11,524

Figure 20. Volumetric flow rate split in the cooling panel for Flownex and RELAP results (*Re* = 2,409 and *Re* = 11,524).

5.3. Sensitivity Analysis for Power Reduction

Pehlivan [11] performed a sensitivity analysis using the *Re* = 2,409 case of Data Set 2. His objective was to learn the impact of power reduction on both riser's temperature profile and first loop bulk volumetric flow rate. To this end, he simulated the WRCCS in RELAP for the steady-state condition decreasing the Net Power by 20% and 10% of the nominal power.

Here, the same procedure Is adopted in Flownex WRCCS model and the results from both codes regarding the bulk volumetric flow rate and risers' temperature profiles are compared. The same pressure drop and other setup configurations from the nominal power (*Re* = 2,409 from Table 4) are maintained for the reduced power simulations.

Table 8 shows the bulk volumetric flow rate results for all net power conditions.

Table 8. Sensitivity analysis results from RELAP and Flownex.

Parameter	First Loop Volumetric Flow Rate (lpm)		
	RELAP	Flownex	Relative difference
Nominal Power	8.15	8.20	0.61%
90% Net Power	7.83	7.76	0.89%
80% Net Power	7.49	7.42	0.93%

It is seen that both codes present the same outcome for all power setups. The accuracy achieved from these results is reasonable, considering that the Flownex secondary losses are assumed to remain the same as the nominal power case to run the reduced power analysis. Thus, for a small range of variation in power, it is observed there is a linear trend between power and volumetric flow rate (Figure 21), as Pehlivan [11] concluded in his studies.

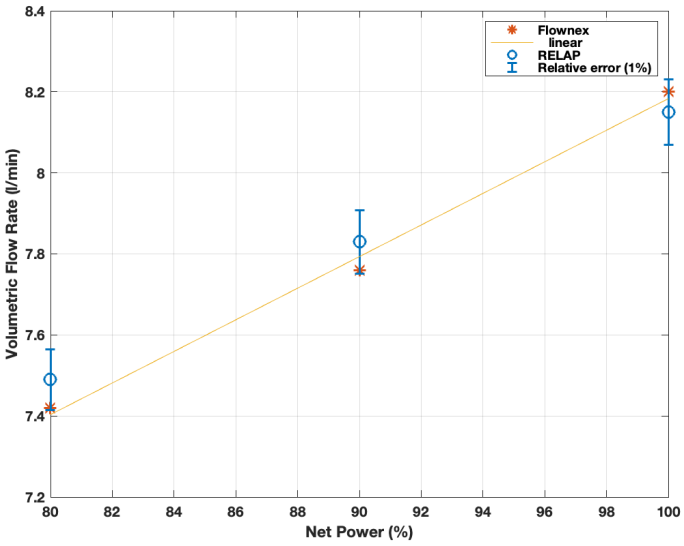

Figure 21. RELAP and Flownex relationship between flow rate and power.

The risers' temperature profile from RELAP and Flownex are presented in Figure 22. The comparison is evaluated by levels for all risers.

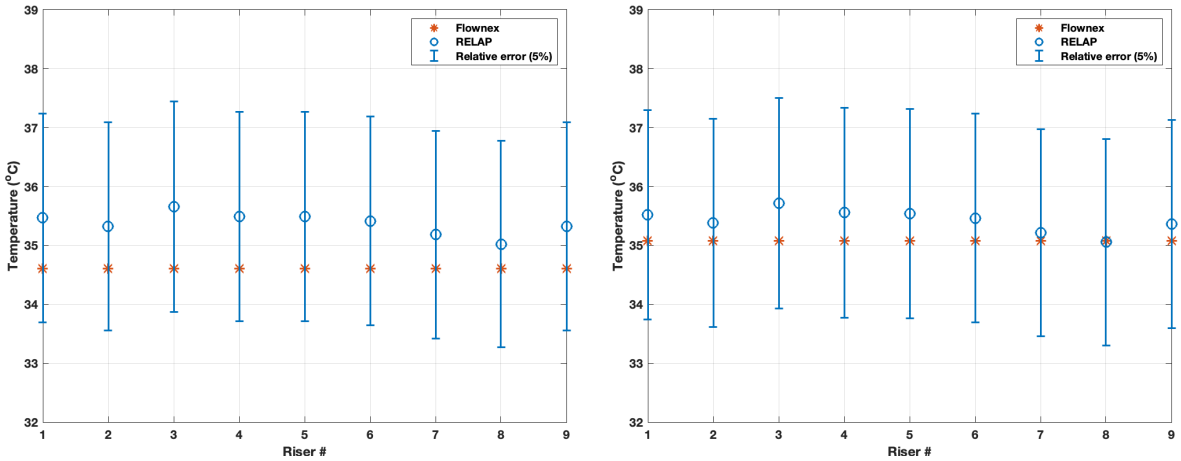

(a1) Level 1 - 80% Net Power (b1) Level 1 - 90% Net Power

Figure 22. Risers' temperature comparisons by level between Flownex and RELAP results.

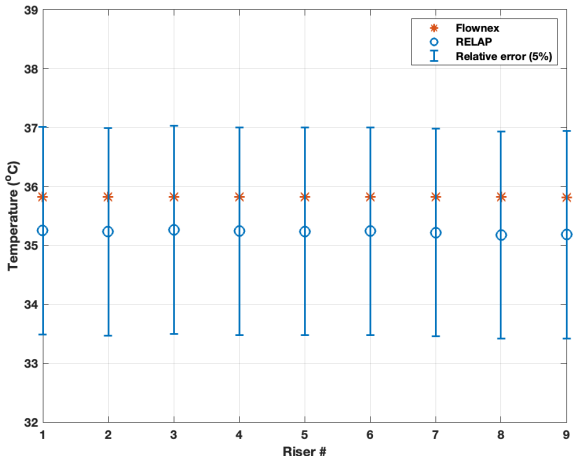

(a2) Level 2 - 80% Net Power

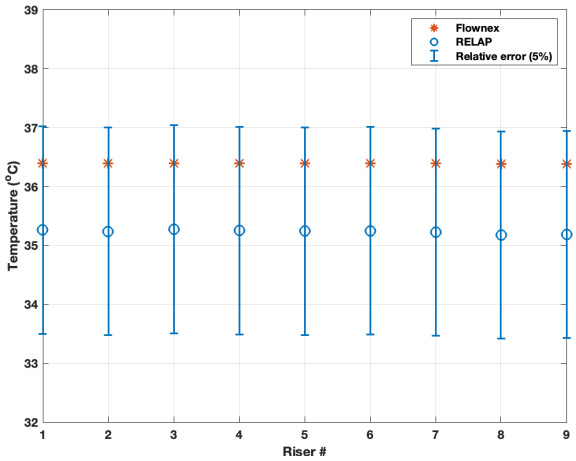

(b2) Level 2 - 90% Net Power

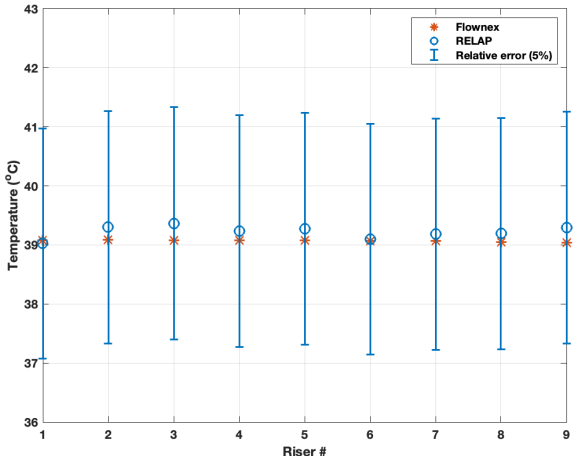

(a3) Level 3 - 80% Net Power

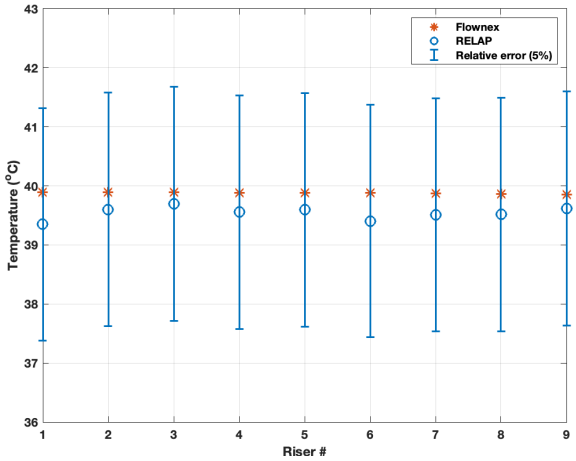

(b3) Level 3 - 90% Net Power

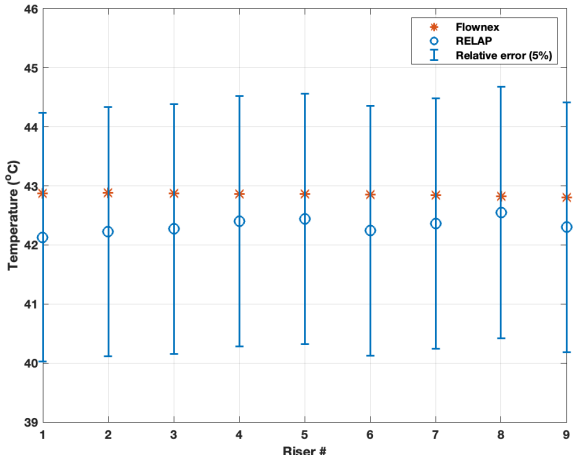

(a4) Level 4 - 80% Net Power

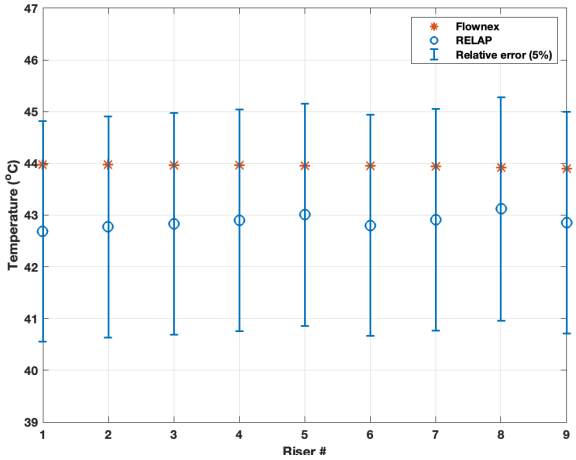

(b4) Level 4 - 90% Net Power

Figure 22. Continued.

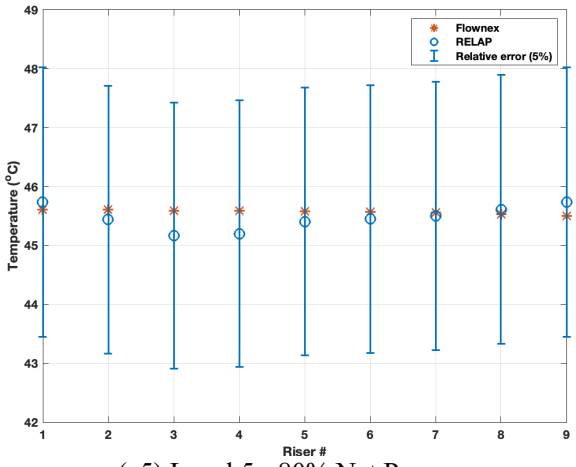

(a5) Level 5 - 80% Net Power

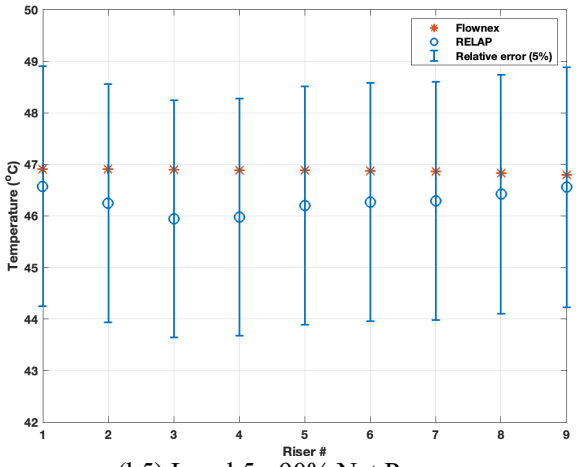

(b5) Level 5 - 90% Net Power

Figure 22. Continued.

The results show that Flownex temperature prediction for both decreased power cases differ from the RELAP ones in less than 5%. Figure 23 condenses the results by plotting the relative error between RELAP and Flownex results.

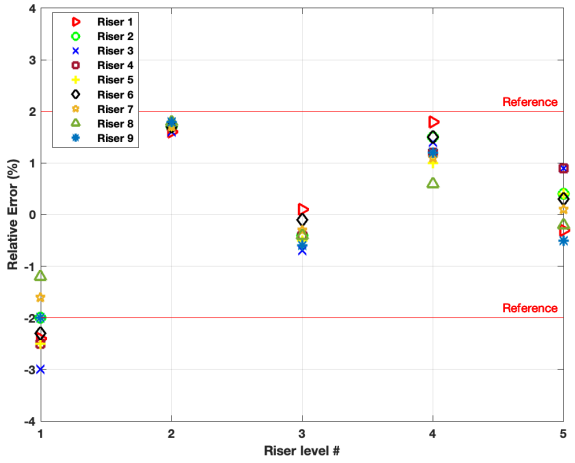

(a) 80% Net Power

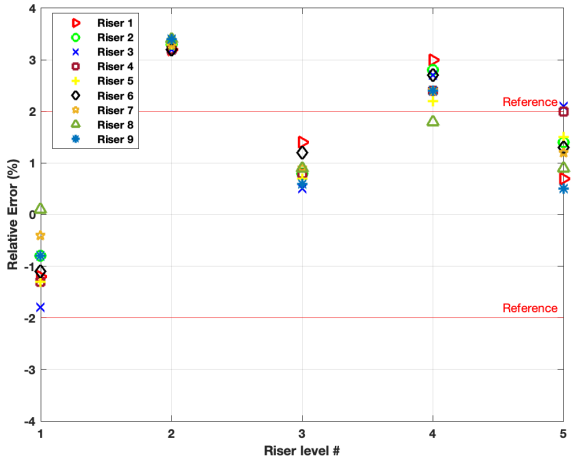

(b) 90% Net Power

Figure 23. Temperature difference between Flownex and RELAP simulation results.

5.4. Loss of Secondary Coolant Scenario

An important analysis to be concerned with in RCCS systems refers to the loss of the secondary coolant, which imparts the capability of cooling down the water in the tank. It leads to an increase in the water temperature circulating in the primary loop of the system until saturation. From this point, two-phase flow phenomena will occur throughout the RCCS facility [21].

Vaghetto et al [22] addressed a study in the TAMU WRCCS focusing on the flow behavior in two-phase condition using high-resolution measurements of the void fraction. They observed that for subcooled boiling conditions, the void fraction was lower than 0.3. Also, the flow was stable, and it had a symmetric distribution across the risers. However, when saturation conditions were reached, unstable, asymmetric flow was found, and the void fraction went up to 0.9. Stagnation and reverse flow were observed as well for this unstable condition.

To verify the capability of system-level codes to predict such behavior in the facility, Pehlivan et al [17] performed a loss of secondary scenario using the RCCS RELAP model. He observed instabilities in flow rate and temperature in the cooling panel similar to the ones encountered in the literature.

Here, Flownex is used for the same purpose. However, the two-phase model built-in in Flownex is the homogenous mixture [20]. This model considers that liquid and vapor are uniformly mixed and thus it does not predict any of the fluctuation behavior captured by the RELAP simulation.

Nonetheless, the global behavior in terms of average parameter values follows the RELAP outcome regarding the cavity inlet temperature, cavity outlet temperature, and bulk volumetric flow rate through the system.

Figure 24 shows these parameters for the Flownex simulation.

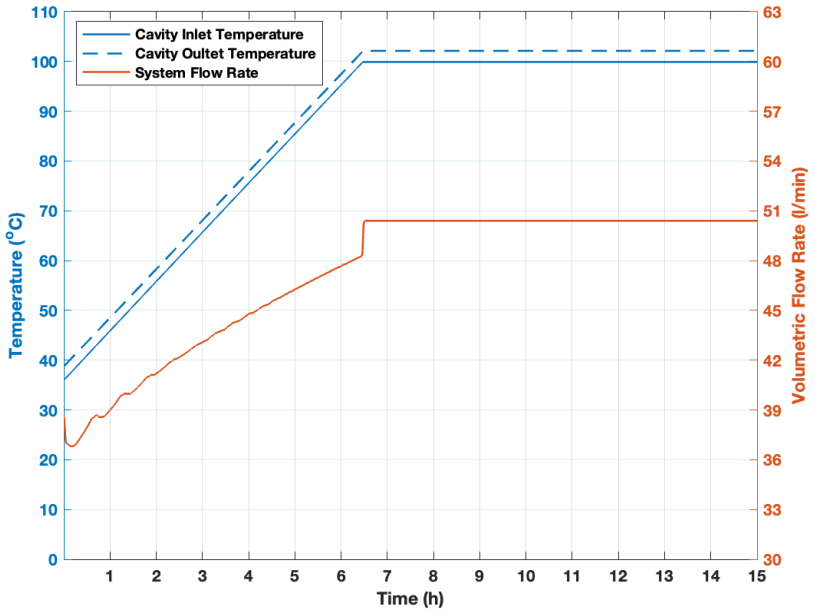

Figure 24. Two-phase flow analysis for loss of the secondary coolant.

6. CONCLUSION

The WRCCS experimental facility was modeled and simulated for three steady-state operational conditions using Flownex (*Re* = 2,409, *Re* = 2490, and *Re* = 11,524 cases). Also, the *Re* = 2,490 case was used to perform a sensitivity analysis for the power reduction and the *Re* = 11,524 case was run without the secondary coolant.

The comparison of the simulation results against the experimental data and previous RELAP simulations demonstrates that the flow and temperature distribution agrees with previous studies ([7]- [9], [11]). For *Re* =11,524, Riser 9 is the coldest riser which corresponds to the highest flow rate, while in Riser 1 the opposite occurs. For both lower *Re* cases, flow and temperature are evenly distributed in the cooling panel. The average relative error of the volumetric flow rate split results between RELAP and Flownex is less than 10% for Data Set 1 and less than 5% for Data Set 2. Combining all cases, more than 70% of Flownex temperature predictions are within the uncertainty of the thermocouple in the experimental facility.

The sensitivity analysis results were compared against the same study carried out by Pehlivan et al [17]. Both codes provided the same result regarding the bulk volumetric flow rate in function of each reduced power case. The relative error was less than 1%.

Although the two-phase model used in Flownex is not applicable to analyze the detailed behavior of the facility for accident scenarios, the results for the average parameters of the bulk volumetric flow rate, inlet and outlet temperature of the cooling panel, show the same trend as the ones predicted by Pehlivan et al [17] using RELAP.

Thus, the overall results show that Flownex is capable of predicting the behavior of the complex fluid flow network of the WRCCS under natural circulation.

In a system-level analysis, the main advantage of running the code comes from its easy setup and fast execution.

Further experiments and simulations efforts can be studied to improve the heat distribution model and fully assess pressure drops throughout the facility.

7. REFERENCES

[1] IEA, "World Energy Outlook 2021," IEA, Paris, 2021.

[2] IAEA, "Energy, Electricity and Nuclear Power Estimates for the Period up to 2050, Reference Data Series No. 1," IAEA, Vienna, 2020.

[3] U.S. DOE Nuclear Energy Research Advisory Committee and the Generation IV International Forum, "A Technology Roadmap for Generation IV Nuclear Energy Systems," 2002.

[4] G. Locatelli, M. Mancini and N. Todeschini, "Generation IV nuclear reactors: Current status and future prospects," *Energy Policy,* vol. 61, pp. 1503-1520, 2013.

[5] J. Thielman, P. Ge, Q. Wu and L. Parme, "Evaluation and optimization of general atomics' gtmhr reactor cavity cooling system usin an axiamotic design approach," *Nuclear Enginnering and Design,* vol. 235, no. 13, pp. 1389-1402, 2005.

[6] L. J. Lommers, F. Shahrokhi, J. A. Mayer and F. H. Southworth, "AREVA HTR Concept for Near-Term Deployment," *Nuclear Engineering and Design,* vol. 187, pp. 282-296, 2012.

[7] N. R. Quintanar, "Temperature and High Resolution Velocity Measurements of Natural Circulation Flow in a Scaled Water Reactor Cavity Cooling System (WRCCS)," Doctoral dissertation, Texas A&M University, 2019.

[8] R. Vaghetto, "Experimental and Computational Study of a Scaled Reactor Cavity Cooling System," Texas A & M University, 2013.

[9] D. M. Holler, "Evaluation and Quantification of Optic Fiber Distributed Sensor Response in Air and Water Environments," Doctoral dissertation, Texas A&M University, 2019.

[10] M. Gorman, E. I. Koyluoglu, R. Vaghetto and Y. A. Hassan, "Reactor Cavity Cooling System Computational Fluid Dynamic Analysis," in *Transactions Of The American Nuclear Society*, 2021.

[11] M. Pehlivan, "Investigation of the Reactor Cavity Cooling System Experimental Facility with RELAP5/SCDAPSIM System Code," Master's thesis, Texas A&M University, 2021.

[12] M-Tech Industrial, "Flownex SE Version 8.14.0.4675 (2022)," [Online]. Available: https://www.flownex.com.

[13] M-Tech Industrial, *Flownex General User Manual,* M-Tech Industrial, 2022.

[14] P. Rousseau, C. du Toit, J. Jun and J. Noh, "Code-to-code comparison for analysing the steady-state heat transfer and natural circulation in an air-cooled RCCS using GAMMA+ and Flownex," *Nuclear Engineering and Design,* vol. 291, pp. 71-89, 2015.

[15] C. G. du Toit, "Fundamental evaluation of the effect of pipe diameter, loop length and local losses on steady-state single-phase natural circulation in square loops using the 1D network code Flownex," *Thermal Science and Engineering Progress,* vol. 22, 2021.

[16] N. R. Quintanar, T. Nguyen, R. Vaghetto and Y. A. Hassan, "Natural circulation flow distribution within a multi-branch manifold," *International Journal of Heat and Mass Transfer,* vol. 153, pp. 1-15, 2019.

[17] M. Pehlivan, A. Vanni, R. Vaghetto and Y. A. Hassan, "Simulations of the Scaled Reactor Cavity Cooling System Experimental Facility with RELAP5/SCDAPSIM System Code," in *Transactions of the American Nuclear Society*, 2021.

[18] K. Hanna, K. Bornoff, J. Murray, M. Jenkins, M. Greutzmacher and D. Kolak, "1D-3D CFD and 3D-1D CFD: Simulation Based Characterization," in *NAFEMS World Congress*, Stockholm, 2017.

[19] G. P. Greyvenstein, "An implicit method for the analysis of transient flows in pipe networks," *International Journal for Numerical Methods in Engineering,* vol. 53, no. 5, pp. 1127-1143, 2002.

[20] M-Tech Industrial, *Flownex Theory Manual,* M-Tech Industrial, 2022.

[21] L. Lommers, B. Mays and F. Shahrokhi, "Passive heat removal impact on AREVA HTR design," *Nuclear Engineering Design,* vol. 271, pp. 569-577, 2014.

[22] R. Vaghetto, S. Yang, D. Hodge and Y. Hassan, "Two-phase flow measurements and observations in a cooling panel of the reactor cavity cooling system," *Progress in Nuclear Energy,* vol. 131, p. 103578, 2021.